Characterizing Bone Microarchitecture and Histology in the G610C Osteogenesis Mouse Model

Dominique Joseph[1], Catherine Omosule[1], Victoria Gremminger[1], Youngjae Jeong PhD[1], Ferris Pfeiffer PhD[2], Charlotte L. Phillips PhD[1, 3]

Departments of Biochemistry[1], Biomedical, Biological and Chemical Engineering[2], and Child Health[3], University of Missouri, Columbia, MO 65211

Introduction

Osteogenesis imperfecta (OI), also known as brittle bone disease, is an incurable connective tissue disorder primarily due to mutations in the type I collagen genes and is clinically manifested in type I collagen-containing tissues, such as bone (1,2). This disorder is associated with bone fragility, skeletal deformities, and growth deficiencies.

Anti-resorptive drugs, bisphosphonates, are currently the standard of care for OI. Although bisphosphonates have been shown to increase bone mass, they inhibit osteoclast activity which are detrimental to bone remodeling, particularly in children. There is no cure for OI, and current treatment options can provide benefit, but may also result in side effects in patients. Thus, there is a need for substitutive treatment methods to improve bone strength and quality in OI.

The Sillence classification system identifies 4 main types of OI ranging from mild to severe in humans, with type I being mild; type II, perinatally lethal; type III, severely deforming; and type IV moderately deforming. To study OI, we employ the Amish *G610C* OI mouse model. Heterozygote *G610C* mice have a glycine to cysteine codon change in the pro-α2(I) chain of type I collagen, and model mild to moderate human OI (type I/IV) (3).

Another murine model used to model human OI is the OI murine (*oim*) model. Homozygote *oim* mice have a spontaneous functional null mutation in the pro-α2(I) chain of type I collagen and exhibit phenotypic and biochemical features typical of the more debilitating, nonlethal form of severe type III human OI (4). In previous studies, the *oim* model demonstrated sex differences in bone microarchitecture, biomechanical properties, and biochemical composition (5). Specifically, male *oim* mice were found to have significantly larger amounts of bone as compared to genotype matched females. Consequently, homozygote females were found to have higher bone fragility, and exhibited decreased moments of inertia.

In this study, we sought to further characterize and compare growth rates, body tissue composition, and bone histological, microarchitectural and biomechanical properties of male and female *G610C* OI mice. Here, we compared properties across both sex and genotype.

We hypothesize that bone growth rates and properties in *+/G610C* mice would show similar sex differences as described in the previous study with *oim* mice. Additionally, we hypothesize that differences will be seen between wildtype (WT) and *+/G610C* mice as well.

Figure 1: OI classification in Humans

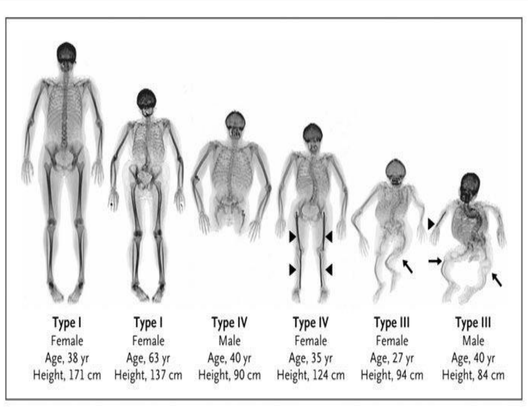

Figure 1: The Sillence classification of osteogenesis imperfecta. The Sillence classification system identifies four main types of OI ranging from mild to severe with type I being mild; type II, perinatally lethal; type III, severely deforming, and type IV moderately deforming. **https://www.nejm.org/doi/full/10.1056/nejmicm062996**

Figure 2: +/G610C Collagen Mutation

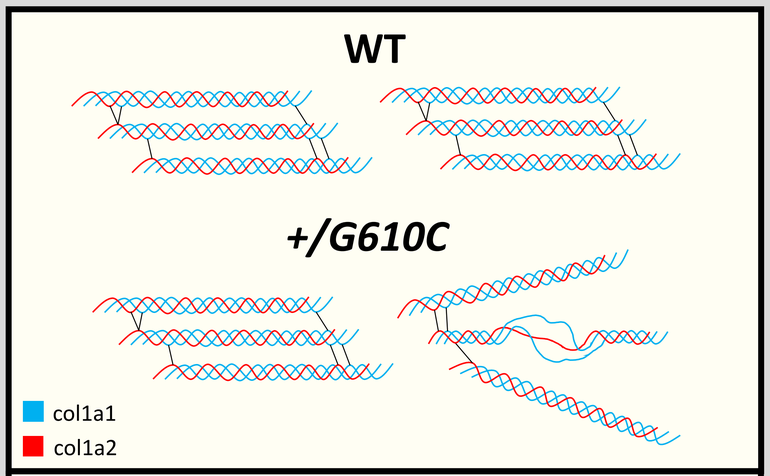

Figure 2: Representation of the heterozygous G610C collagen mutation. The G610C mouse models a COL1A2 gene mutation seen in a large Amish kindred. The heterozygous G610C murine mutation results in a glycine to cysteine substitution in the α2(I) chain. This mutation disrupts trimer folding and collagen–collagen trimer interactions.

Methods

Breeding: Wildtype (WT) and heterozygous (+/*G610C*) G610C male and female mice were generated from +/*G610C* and WT crosses. Weaning was performed at three weeks of age. Mice were weighed weekly. Heterozygous (9 male, 9 female) and WT (9 male, 11 female) mice were euthanized at 4 months of age for tissue harvest and analyses.
Bone Microarchitecture: Right femora were excised, cleaned off soft tissues and stored in 1X PBS at -20°C until analyses. Right femoral trabecular and cortical microarchitecture was investigated by vivaCT 40 µCT scan analyses (SCANCO Medical AG, Bassersdorf, Switzerland). Data was analyzed using the SCANCO Medical microCT software system.
3 Point Bending: After uCT analyses, right femora underwent 3 point bending tests using the Stable Micro Systems TA-HDi Texture Analyzer (Texture Technologies Corp), software-version 07.14H. Bones were placed anterior-posteriorly on support stands placed 9 mm apart. Testing was performed with a load cell weight of 5 kg set on an automatic trigger force of 0.2N and a constant speed of 0.02mm/sec until bone failure. Stiffness and work-to-fracture were determined from the load displacement curve using Microsoft Excel.

Figure 3: Body Weights

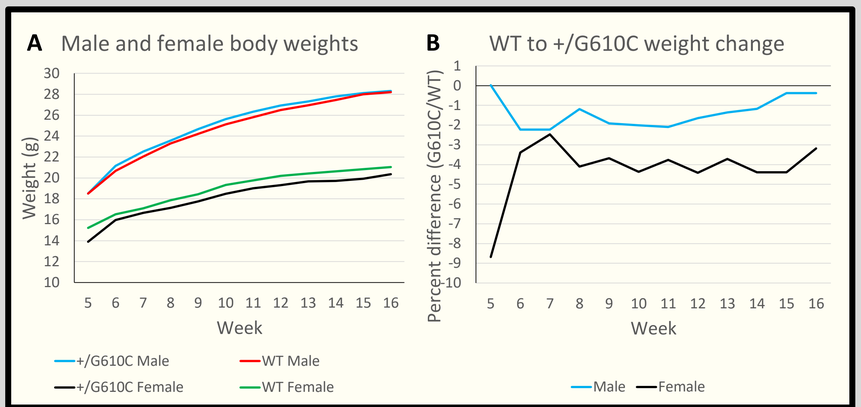

Figure 3. Weekly body weights of *+/G610C* and WT males and females over 12 weeks (A) and percent differences (G610C/WT) within sex (B). Males present with consistently higher weights and lower difference between genotypes than females. Females began with a significantly larger difference between WT and +/G610C than males at 5 weeks of age, though this difference decreased by 6 weeks of age. n=9-11

Figure 5: Muscle Weights

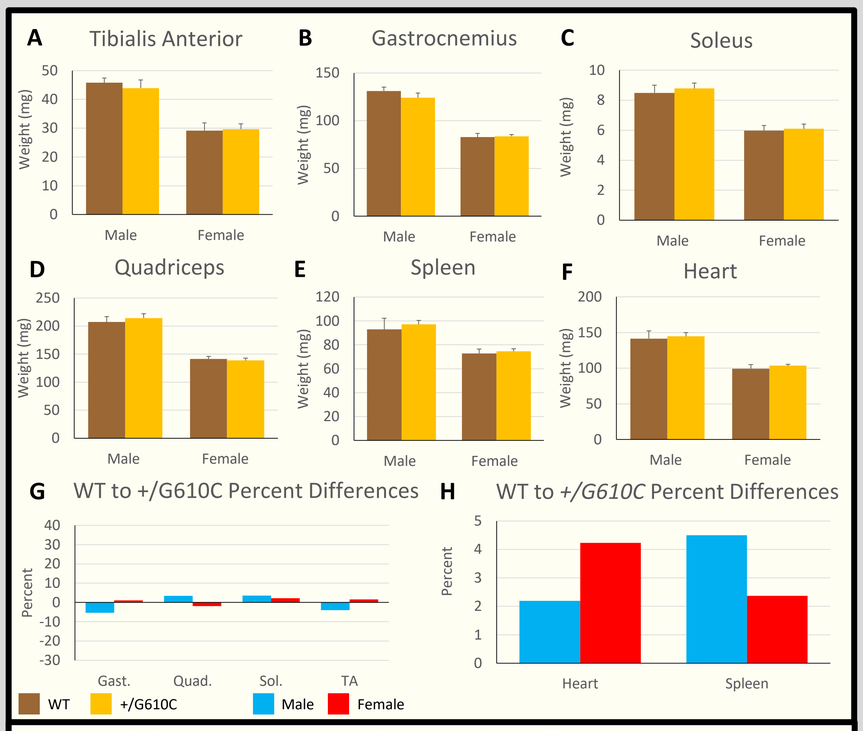

Figure 5. Hindlimb skeletal muscle weights show no significant differences across genotypes or sex. The spleen and heart are known to contain large quantities on col1a1. Thus, they have been predicted to be impacted by +/G610C mutations. Here, both male and female +/G610C mice display minor increases of heart and spleen weights. * p<0.05 as compared to sex matched wildtype. Values are mean ± SD; n= 9-11

Figure 4: Bone Microarchitecture and Strength

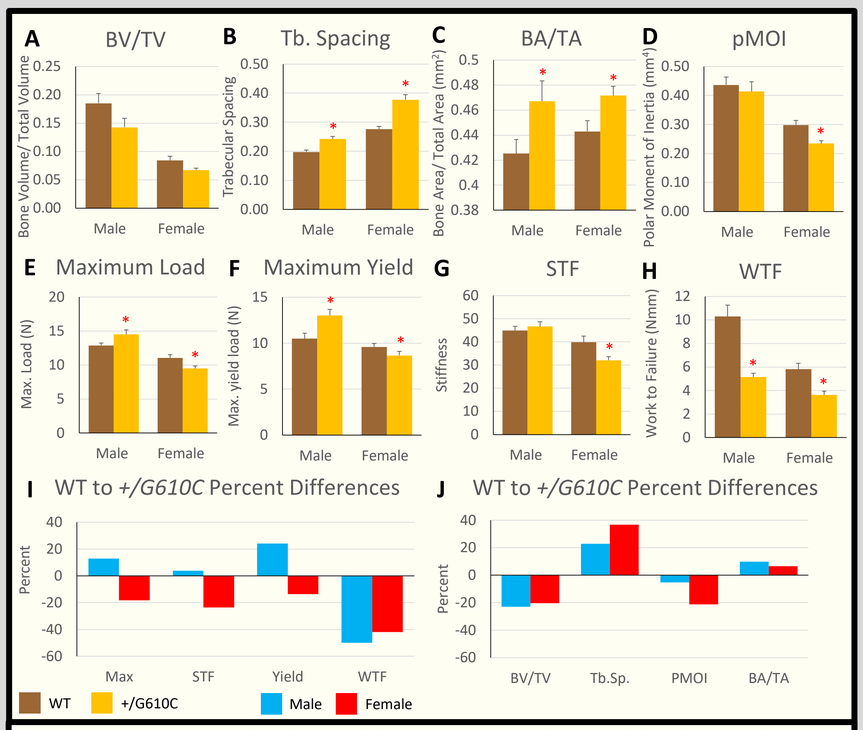

Figure 4. µCT cortical and trabecular morphological parameters of proximal tibiae from WT (11 females, and 9 males) and *+/G610C* (9 females, and 9 males) mice. Both males and females display increases of trabecular spacing and bone area to total area (BA/TA) ratios, as well as decreases of polar moment of inertia (pMOI) and trabecular bone volume to total volume ratios in *+/G610C* relative to WT mice. Females present with larger decreases of strength parameters from WT to *+/G610C*, though males display a slightly higher decrease in work to fracture (WTF) values from WT to *+/G610C*. * p<0.05 as compared to WT genotype. Values are mean ± SD; n= 9-11

Figure 6: Osteoclast Imaging

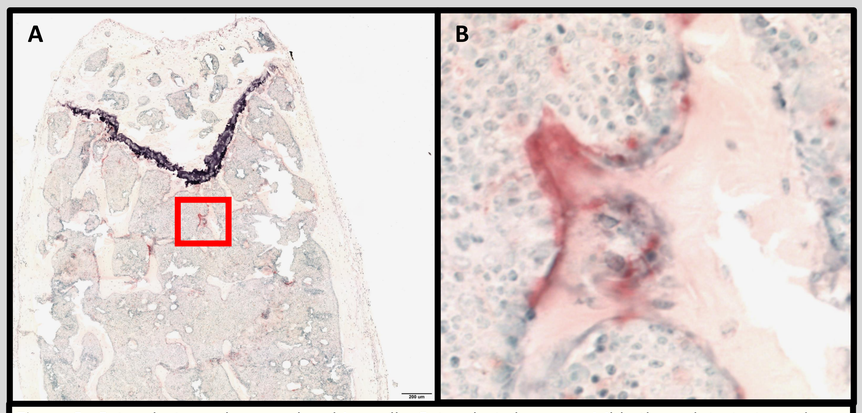

Figure 6. Osteoclasts are bone reabsorbing cells. Osteoclasts become visible through tartrate acid resistant phosphatase (TRAP) staining where they appear as multinucleated cells lining mineralized bone surface areas. Histomorphometric analyses of static parameters performed using ImageJ and will give osteoclast number and activity.
Original lab photo: Wildtype tibia 14G5257.

Conclusions

Although *+/G610C* male and female mice have similar body weights as their WT counterparts, femoral bone microarchitecture is compromised as evidenced by decreased bone volume over total bone volume (BV/TV) and polar moment of inertia (PMOI); and increased trabecular spacing (Tb.Sp). Bone biomechanical strength is also decreased in both male and female *+/G610C* mice. While only female *+/G610C* mice displayed decreases in femoral maximal load, yield load, and stiffness relative to their WT counterparts, both male and female *+/G610C* mice present with greater than 42% reductions in work to fracture values. Male and female *+/G610C* mice present with similar trends in overall bone and muscle weight decreases. Overall data suggests that though there are genotypic bone microarchitecture differences, sex differences may be less prevalent in the *G610C* mouse model than in the *oim* model.

Future Work

Bone is composed of three major cell types: osteoblasts, osteoclasts, and osteocytes. Osteoblasts secrete matrix for bone formation, osteoclasts absorb bone tissue, and osteocytes are osteoblast derived cells which act as mechanosensors. Histological analyses of osteoblast and osteoclast number and function are currently underway to define their cellular contribution to compromised *G610C* bone. We hypothesize that reduced bone in *+/G610C* models is due to coupling of reduced osteoblast numbers and increased osteoclasts numbers.

References

1. Carriero, Alessandra, et al. "Animal Models of Osteogenesis Imperfecta: Applications in Clinical Research." *Orthopedic Research and Reviews*, Volume 8, 2016, pp. 41–55., doi:10.2147/orr.s85198.
2. Forlino, Antonella et al. "New perspectives on Osteogenesis imperfecta" *Nature reviews. Endocrinology* vol. 7,9 540-57. 14 Jun. 2011, doi:10.1038/nrendo.2011.81
3. Masci, Marco et al. "Bone mineral properties in growing Col1a2(+/G610C) mice, an animal model of osteogenesis imperfecta." *Bone* vol. 87 (2016): 120-9. doi:10.1016/j.bone.2016.04.011
4. Chipman SD, Sweet HO, McBride DJ Jr, et al. "Defective pro alpha 2(I) collagen synthesis in a recessive mutation in mice: a model of human osteogenesis imperfecta" *Proceedings of the National Academy of Sciences of the United States of America*. Mar. 1993, 90(5):1701-1705. DOI: 10.1073/pnas.90.5.1701.
5. Yao, Xiaomei et al. "Gender-dependence of bone structure and properties in adult osteogenesis imperfecta murine model." *Annals of biomedical engineering* vol. 41,6 (2013): 1139-49. doi:10.1007/s10439-013-0793-7

Acknowledgements

NIH NCATS Grant #UL1 TR002345
Leda J. Sears Trust